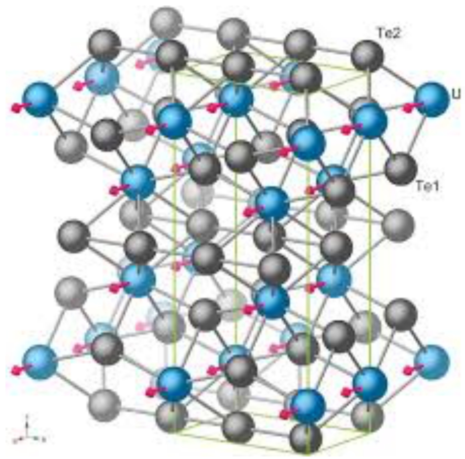


# Spin-Orbit Coupling Induced $j_z$ Degeneracy in Superconducting $UTe_2$

* *Immm (*bco)
- space group #71
- low site symmetry
- U chains along a axis

Warren Pickett[1] and Sasha (A.B.) Shick[2]
[1]University of California Davis
[2]Czech Academy of Sciences, Prague

$UTe_2$: known conventional properties (room temperature & pressure, etc) for some time. Lately studied under more extreme conditions.

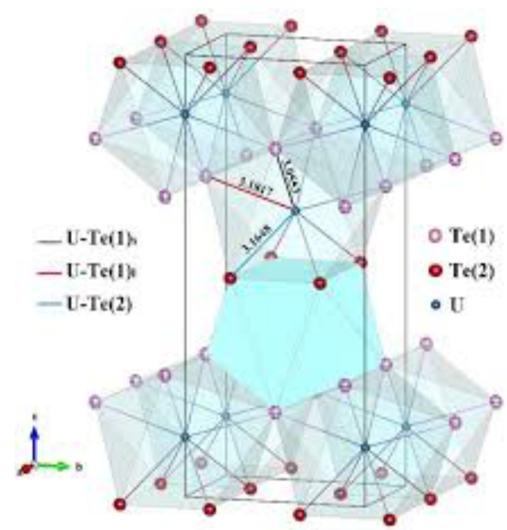

"Correlated Spin-Orbit Coupled [Transition Metal] Oxides" -- why $UTe_2$?

Tutorial on Transition Metal Oxides

| Group → / Period ↓ | 1 | 2 | 3 | 4 | 5 | 6 | 7 | 8 | 9 | 10 | 11 | 12 | 13 | 14 | 15 | 16 | 17 | 18 |
|---|---|---|---|---|---|---|---|---|---|---|---|---|---|---|---|---|---|---|
| 1 | 1 H | | | | | | | | | | | | | | | | | 2 He |
| 2 | 3 Li | 4 Be | | | | | | | | | | | 5 B | 6 C | 7 N | 8 O | 9 F | 10 Ne |
| 3 | 11 Na | 12 Mg | | | | | | | | | | | 13 Al | 14 Si | 15 P | 16 S | 17 Cl | 18 Ar |
| 4 | 19 K | 20 Ca | 21 Sc | 22 Ti | 23 V | 24 Cr | 25 Mn | 26 Fe | 27 Co | 28 Ni | 29 Cu | 30 Zn | 31 Ga | 32 Ge | 33 As | 34 Se | 35 Br | 36 Kr |
| 5 | 37 Rb | 38 Sr | 39 Y | 40 Zr | 41 Nb | 42 Mo | 43 Tc | 44 Ru | 45 Rh | 46 Pd | 47 Ag | 48 Cd | 49 In | 50 Sn | 51 Sb | 52 Te | 53 I | 54 Xe |
| 6 | 55 Cs | 56 Ba | 57 La * | 72 Hf | 73 Ta | 74 W | 75 Re | 76 Os | 77 Ir | 78 Pt | 79 Au | 80 Hg | 81 Tl | 82 Pb | 83 Bi | 84 Po | 85 At | 86 Rn |
| 7 | 87 Fr | 88 Ra | 89 Ac ** | 104 Rf | 105 Db | 106 Sg | 107 Bh | 108 Hs | 109 Mt | 110 Ds | 111 Rg | 112 Cn | 113 Nh | 114 Fl | 115 Mc | 116 Lv | 117 Ts | 118 Og |
| | | | * | 58 Ce | 59 Pr | 60 Nd | 61 Pm | 62 Sm | 63 Eu | 64 Gd | 65 Tb | 66 Dy | 67 Ho | 68 Er | 69 Tm | 70 Yb | 71 Lu | |
| | | | ** | 90 Th | 91 Pa | 92 U | 93 Np | 94 Pu | 95 Am | 96 Cm | 97 Bk | 98 Cf | 99 Es | 100 Fm | 101 Md | 102 No | 103 Lr | |

Tellurium is just (very) heavy oxygen.
Uranium is just a (very) heavy transition metal.

Ergo: $UTe_2$ is a heavy "**transition metal oxide**."

Uranium has very large **spin-orbit coupling**.

# Nearly Ferromagnetic Superconductor $UTe_2$. Likely Non-unitary Triplet Pairing

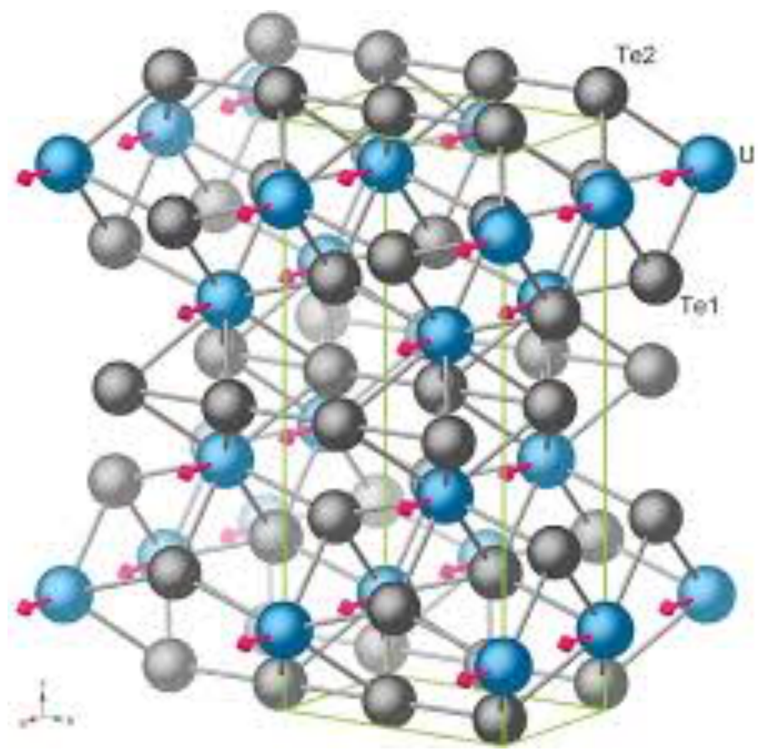


* *Immm (*bco, inversion)
- space group #71
- low site symmetry
- U chains along a axis
- Ising-like moments: [100]

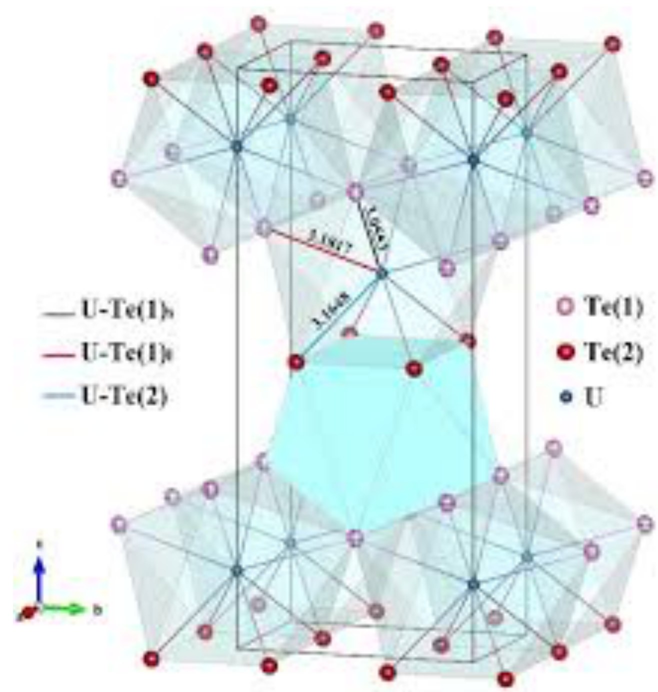

First UMd-NIST arXiv posting was November 2018 (one year ago)

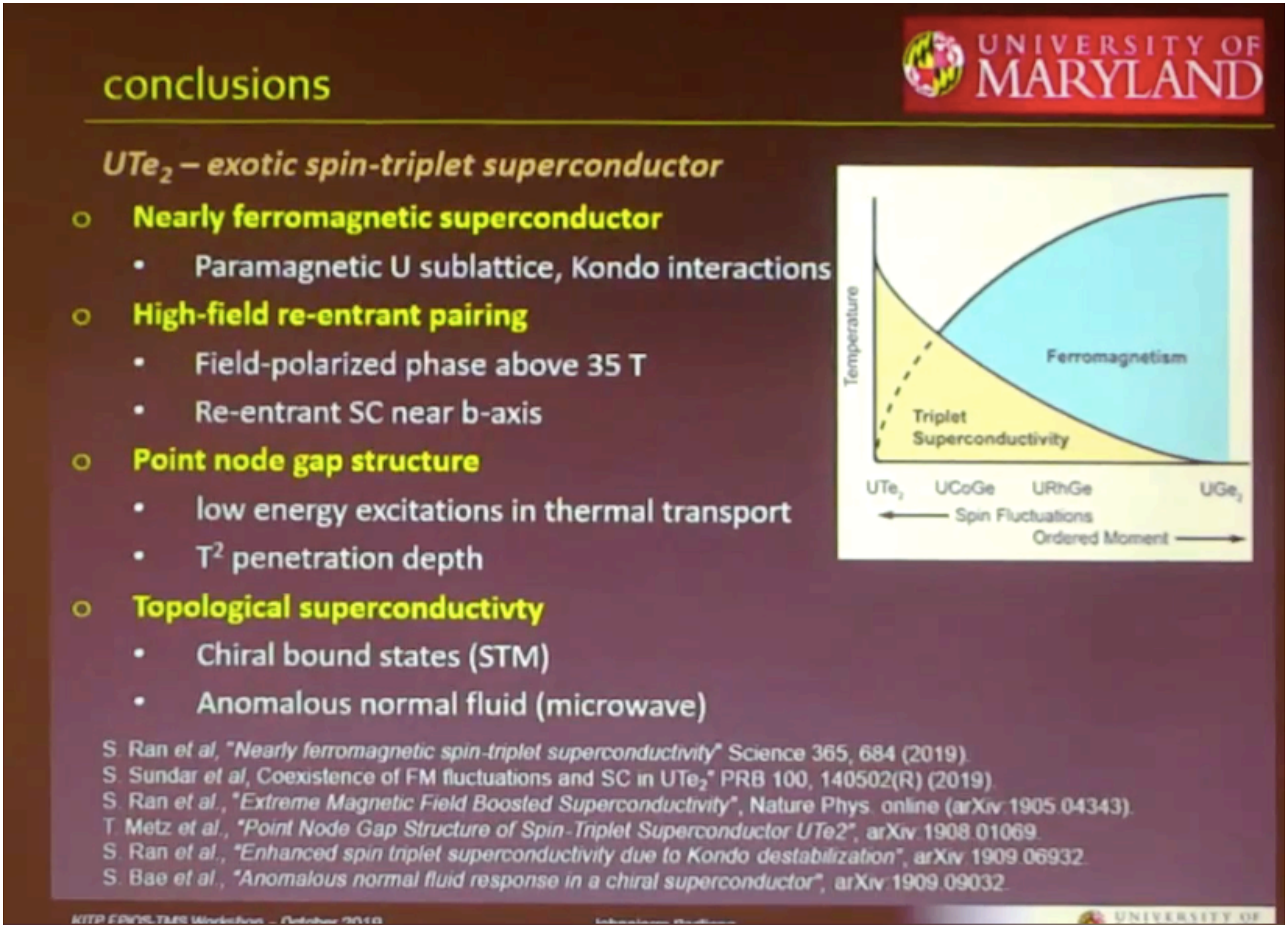


Slide from JP Paglione from talk (online) at KITP, UCSB (2019)
[experimental papers from UMd-NIST on $UTe_2$]

Publications from groups of D. Aoki & J. Flouquet (most published; JPSJ)

arXiv:1905.02998 Metamagnetic Transition in Heavy Fermion Superconductor UTe2 Atsushi Miyake et al.

arXiv:1905.03990 Magnetic-Field-Induced Phenomena in the Paramagnetic Superconductor UTe2. William Knafo et al.

arXiv:1905.05181 Field-reentrant superconductivity close to a metamagnetic transition in the heavy-fermion superconductor UTe2, Georg Knebel et al.

arXiv:1906.01303 125Te-NMR Study on a Single Crystal of Heavy Fermion Superconductor UTe2, Yo Tokunaga et al.

arXiv:1907.03033 Thermodynamic Investigation of Metamagnetism in Pulsed High Magnetic Fields on Heavy Fermion Superconductor UTe2, Shusaku Imajo et al.

arXiv:1907.11118 Fermi-Surface Instabilities in the Heavy-Fermion Superconductor UTe2 Qun Niu et al.

arXiv:1908.09418 Electronic Structure of UTe2 Studied by Photoelectron Spectroscopy Shin-ichi Fujimori et al.

arXiv:1909.06074 Multiple superconducting phases in a nearly ferromagnetic system D. Braithwaite et al.

arXiv:1909.08853 Superconducting Properties of Heavy Fermion UTe2 Revealed by 125Te-Nuclear Magnetic Resonance, Genki Nakamine et al.

Several papers were published **before** the 1st UMd–NIST **publication**

1st arXiv posting, unpubl.

# Spontaneously polarized half-gapped superconductivity

Sheng Ran,[1,2*] Chris Eckberg,[2] Qing-Ping Ding,[3] Yuji Furukawa,[3] Tristin Metz,[2]
Shanta R. Saha,[1,2] I-Lin Liu,[1,2,4] Mark Zic,[2]
Johnpierre Paglione,[1,2] Nicholas P. Butch[1,2*]

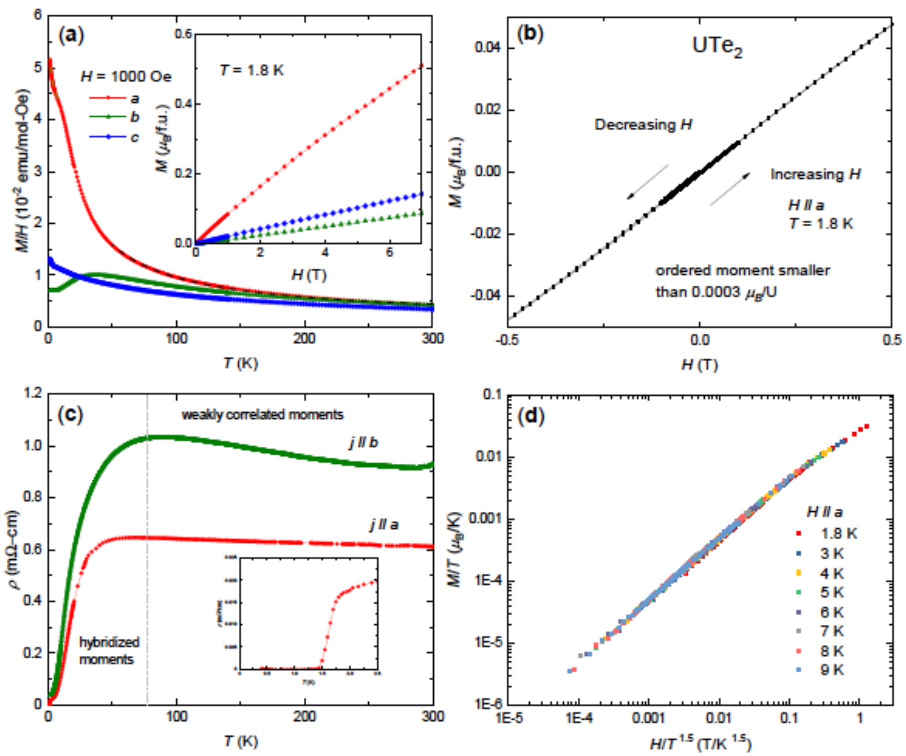


Figure 4: Upper critical field $H_{c2}$ of $UTe_2$. (a)-(c) Color contour plots of resistivity value as a function of temperature and magnetic field, with magnetic fields applied along (a) *a*-axis, (b) *b*-axis and (c) *c*-axis. The current is applied along *a*-axis. (d) The $H_{c2}$ value as a function of $T_c$ in three directions. Dotted lines represent the WHH fit of the $H_{c2}$ data. (e) Temperature dependent resistivity data in magnetic fields applied along *b* axis up to 20 T.

$UTe_2$: early experimental data

- susceptibility: Ising-like; a axis
- no hysteresis (no magnetic order)
- heavy fermion resistivity,
  $T_K$ ~ 50-75K

* (inset) $T_c$ transition

Another anisotropic HF superconductor

1st arXiv posting, unpubl.

# Spontaneously polarized half-gapped superconductivity

Sheng Ran,[1,2*] Chris Eckberg,[2] Qing-Ping Ding,[3] Yuji Furukawa,[3] Tristin Metz,[2]
Shanta R. Saha,[1,2] I-Lin Liu,[1,2,4] Mark Zic,[2]
Johnpierre Paglione,[1,2] Nicholas P. Butch[1,2*]

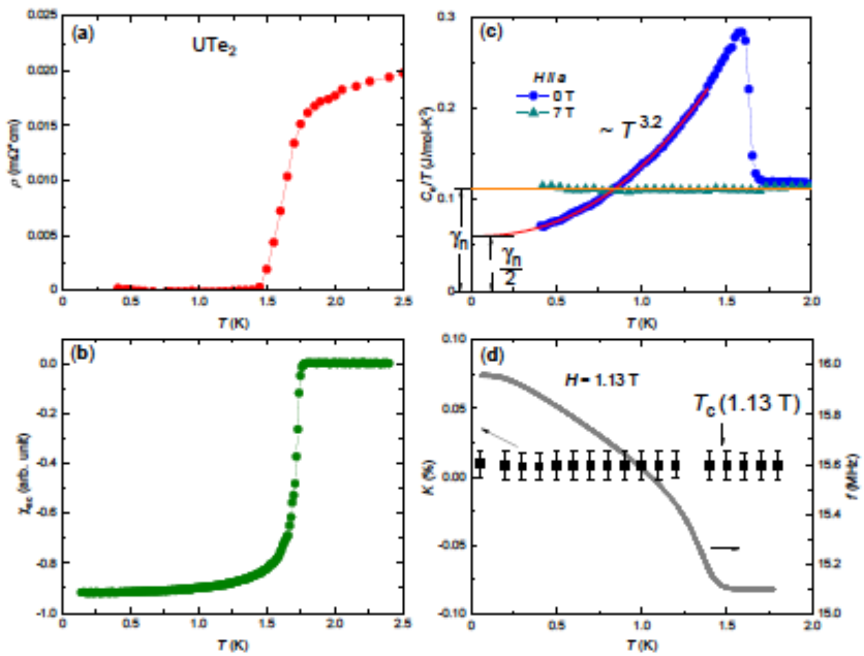


Figure 3: Superconducting state properties of $UTe_2$. Temperature dependence of (a) resistivity and (b) ac magnetization data at low temperatures showing the bulk superconductivity. (c) Electronic contribution to heat capacity (phonon contribution has been subtracted) in zero and 7 T, divided by temperature as a function of temperature to illustrate $\gamma$ in the superconducting and normal states. Magnetic field is applied along $a$-axis. (d) Temperature dependence of $^{125}$Te NMR Knight shift $K$ below and near $T_c$ of powdered $UTe_2$ sample (left axis) and temperature dependence of the resonance frequency $f$ of the NMR tank circuit confirming the superconducting state and $T_c$ (right axis).

## $UTe_2$: early experimental data

- verifying superconductivity
- resistivity drop
- susceptibility shift
- no Knight shift change
- heat capacity transition
- entropy balance – ooops
- residual $C_V/T$ as T→0. Hmmm..

Normal carriers (50%) within the superconducting state. Neither point nodes nor line nodes. But what …?

## Spontaneously polarized half-gapped superconductivity

Sheng Ran,[1,2*] Chris Eckberg,[2] Qing-Ping Ding,[3] Yuji Furukawa,[3] Tristin Metz,[2]
Shanta R. Saha,[1,2] I-Lin Liu,[1,2,4] Mark Zic,[2]
Johnpierre Paglione,[1,2] Nicholas P. Butch[1,2*]

Science, Aug. 2019

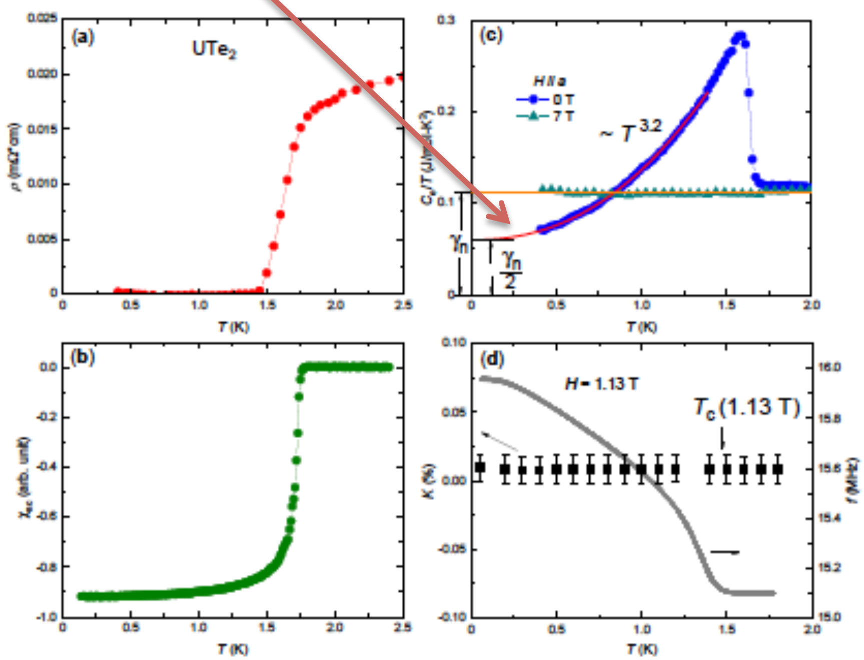


Figure 3: Superconducting state properties of $UTe_2$. Temperature dependence of (a) resistivity and (b) ac magnetization data at low temperatures showing the bulk superconductivity. (c) Electronic contribution to heat capacity (phonon contribution has been subtracted) in zero and 7 T, divided by temperature as a function of temperature to illustrate $\gamma$ in the superconducting and normal states. Magnetic field is applied along *a*-axis. (d) Temperature dependence of $^{125}$Te NMR Knight shift $K$ below and near $T_c$ of powdered $UTe_2$ sample (left axis) and temperature dependence of the resonance frequency $f$ of the NMR tank circuit confirming the superconducting state and $T_c$ (right axis).

$UTe_2$: early experimental data

- verifying superconductivity
- resistivity drop
- susceptibility shift
- no Knight shift change
- heat capacity transition
- $\gamma$ = 120 mJ/mol-K$^2$ (heavy)
- entropy balance – ooops
- residual $C_V/T$ as T→0. Hmmm..

Normal carriers (50%) within the superconducting state. Neither point nodes nor line nodes. But what …?

**Nodal structure of unconventional superconductors probed by angle resolved thermal transport measurements**

Matsuda, Izawa, Vekhter, J Phys: Cond Matt (2006)

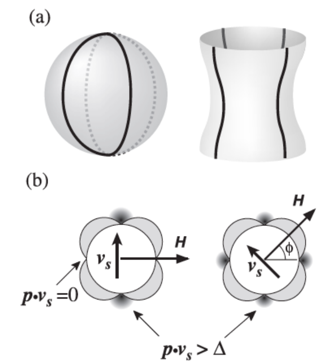


BCS: simple fully gapped Fermi surface

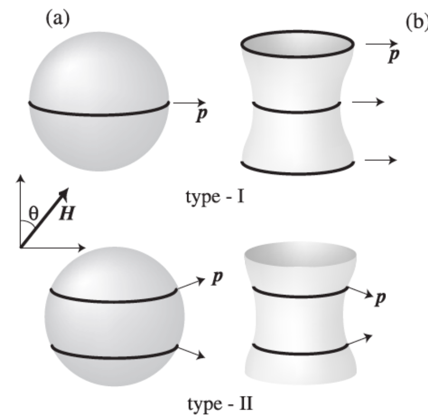


Orientation of the line nodes becomes apparent in their transport properties

Evidence of point gap in $YNi_2B_2C$.
Kamata et al. Physica C 2003


Fig. 1. (a) Angular variation of the $c$-axis thermal conductivity $\kappa_{zz}$ at $H = 1$ T and $T = 0.43$ K (thermal current $q \| c$). $\kappa_{zz}$ are

Examples of line nodes in the superconducting gap on the Fermi surface

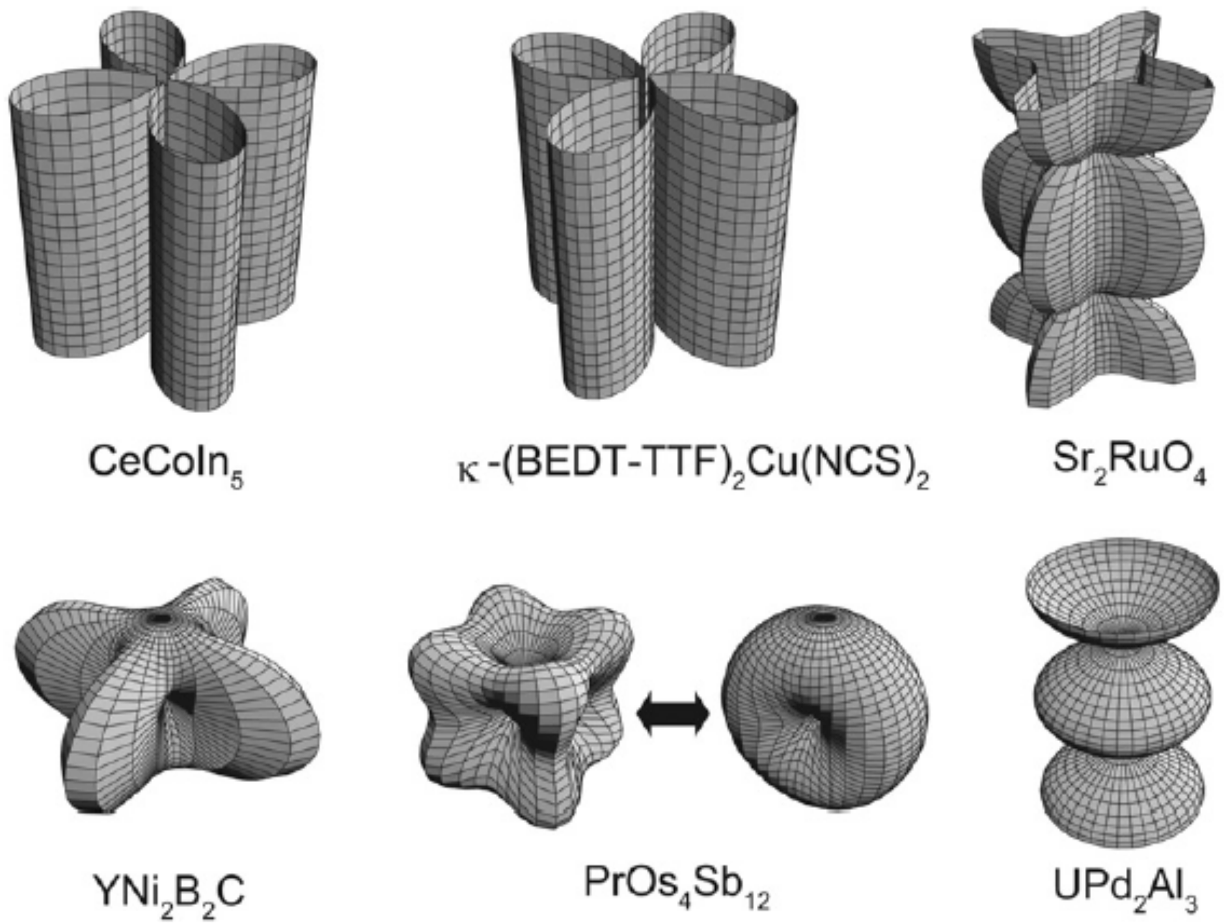


**Figure 35.** The nodal structure of several unconventional superconductors, including quasi-two dimensional heavy fermion $CeCoIn_5$, organic $\kappa$-(BEDT-TTF)$_2$Cu(NCS)$_2$, ruthenate $Sr_2RuO_4$ (the gap structure takes into account additional fourfold modulation as indicated by the specific heat measurements), borocarbide $YNi_2B_2C$, heavy fermion $PrOs_4Sb_{12}$, and heavy fermion $UPd_2Al_3$, which are determined by angular variation of the thermal conductivity.

Matsuda, Izawa, Vekhter, J Phys: Cond Matt (2006)

Superconducting gaps: fully gapped; point nodes; line nodes. That's all. Except…

**Bogoliubov Fermi Surfaces in Superconductors with Broken Time-Reversal Symmetry**

D. F. Agterberg,[1,*] P. M. R. Brydon,[2,†] and C. Timm[3,‡]

PRL

Bogoliubov Fermi surface:
- In the superconducting state, an area of zero gap occurs
- many consequences on properties within the superconducting state

Bogoliubov Fermi surfaces can evolve (vs some parameter) into
- nodal lines in the gap
- point nodes in the gap

before the nodes disappear.

A Bogoliubov Fermi surface could resolve the question of normal excitations below the superconducting critical $T_c$.

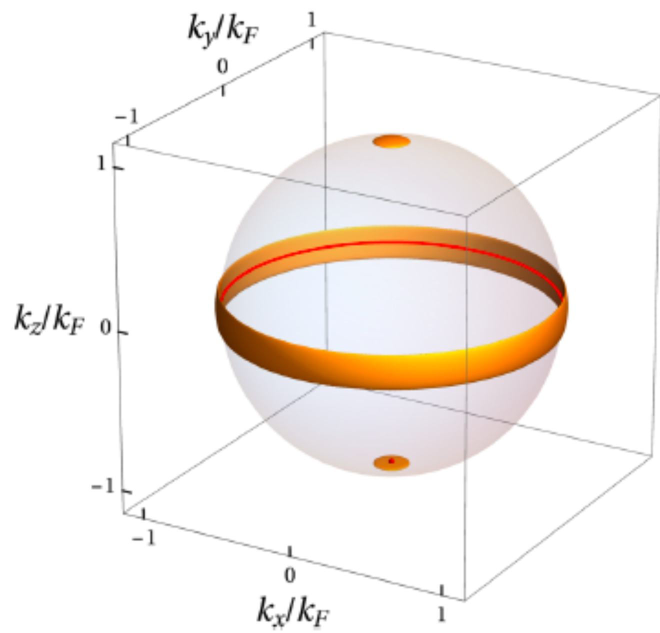


FIG. 1. Bogoliubov Fermi surfaces of the superconducting $k_z(k_x + ik_y)$ state, shown here for the case where only one band

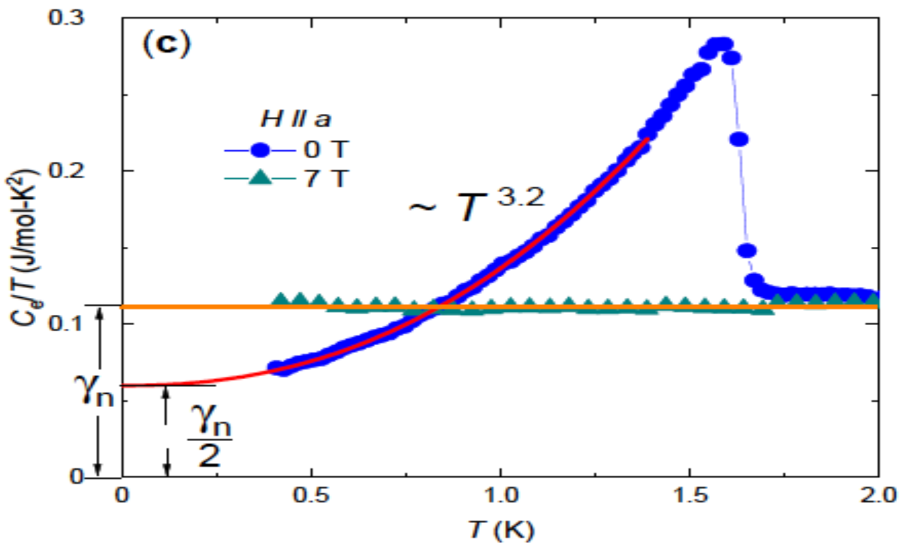


…until additional data appeared

Data down to 0.4K

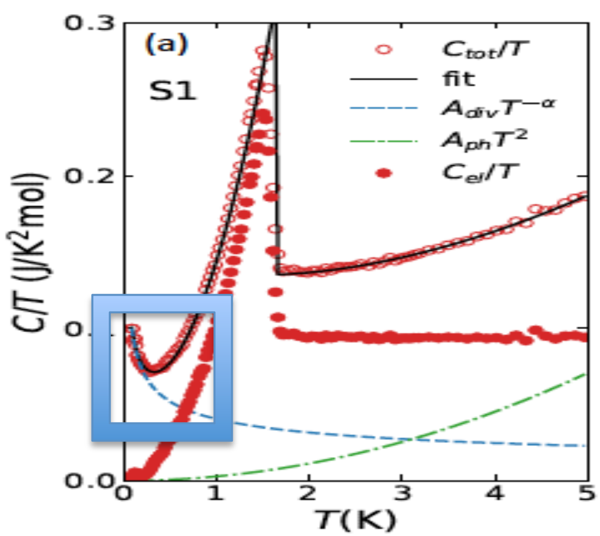


Data down to 0.04K.
An additional source of entropy appears.

$C_V$ data scaled to same T and $C_V/T$ axes.

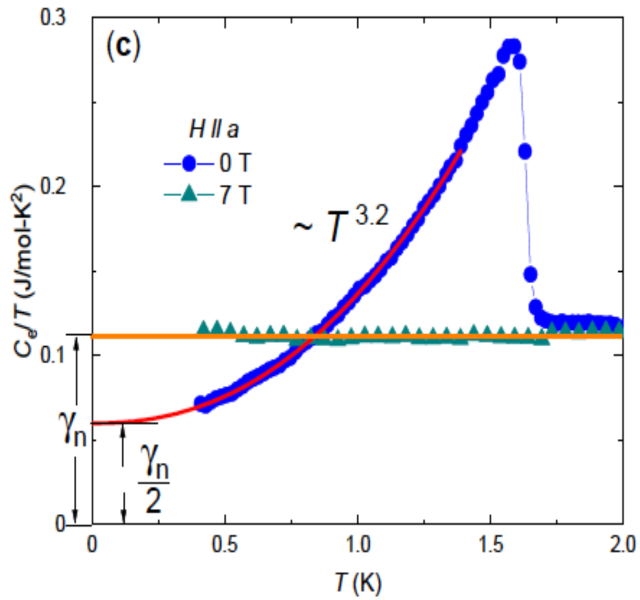


Data down to 0.4K

Data down to 0.04K

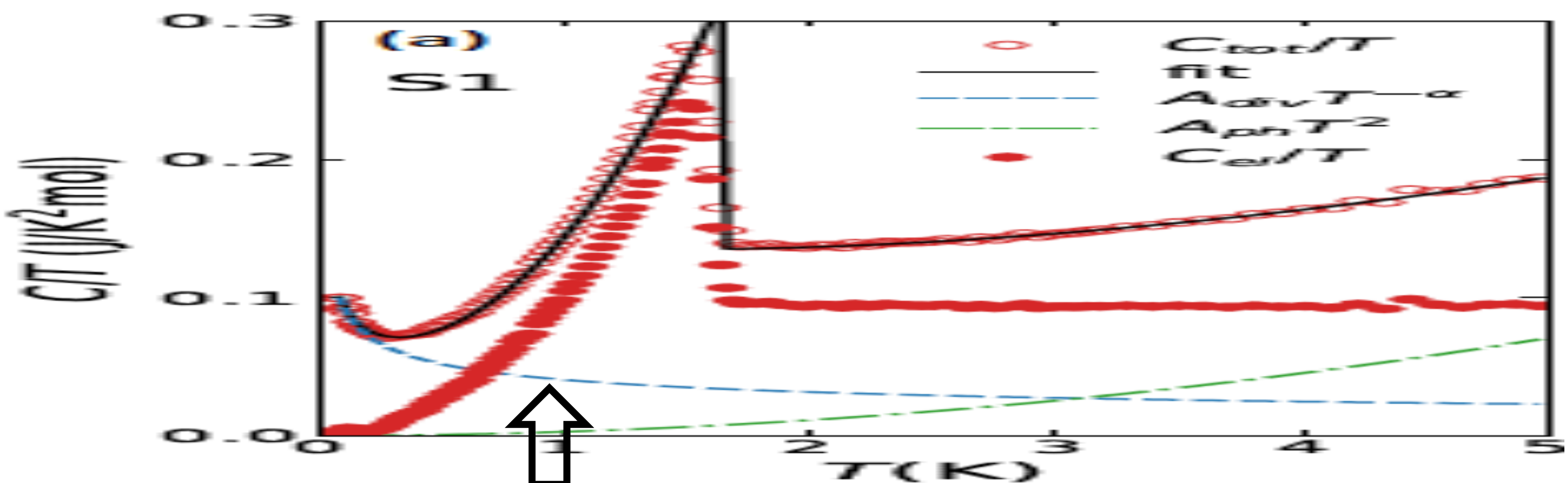


fit to $T^{-1/3}$

# Analyzing the heat capacity data

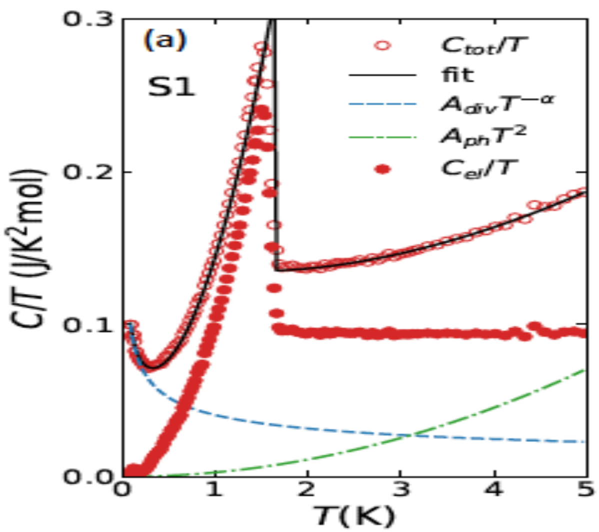


Fit from 50 mK to 5K with

$$\frac{C}{T} = A_{ph}T^2 + A_{div}T^{-\alpha} + \begin{cases} A_{sc}T^2 & T < T_c \\ \gamma_n & T > T_c \end{cases}$$

$\alpha$=0.33-0.35~1/3

Other parameters not published.

An open issue: the $T^{-1/3}$ form gives divergent entropy as T gets large.

# $UTe_2$: Experimental data and analysis

Specific heat: after the fit, $C_v/T \sim T^2$ indicates point node, p-wave gap

The extra excitations/ entropy is assumed unchanged between normal/SC states.

[Does not contribute to thermal conductivity, hence “localized”.]

Metz et al. arXiv:1908:01069

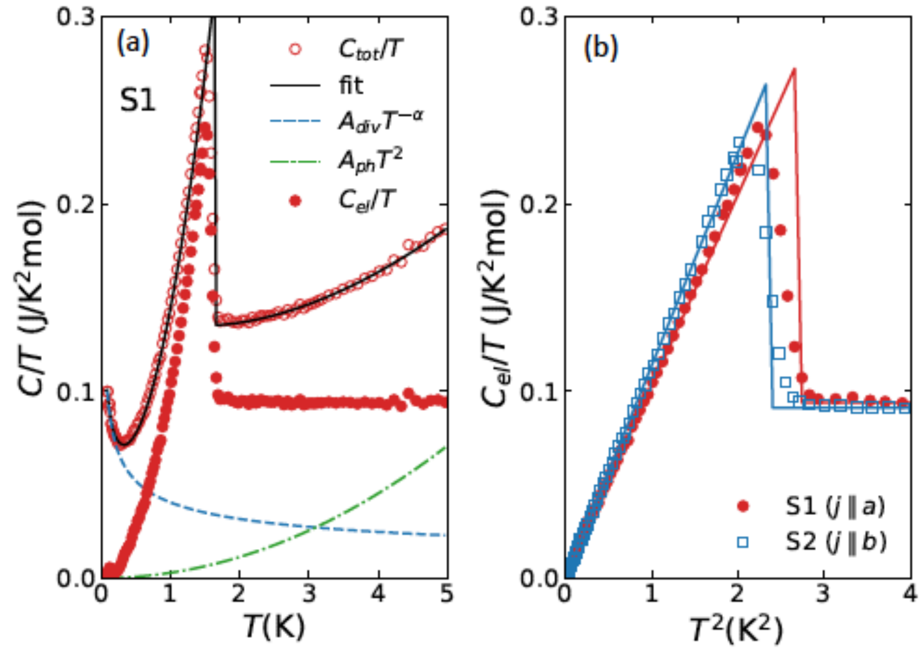


FIG. 1. Analysis of the low temperature heat capacity of $UTe_2$ single-crystal samples S1 and S1 (same crystals used for thermal transport measurements). (a) The total measured heat capacity (open circles) of sample S1 decomposed into a weak power law divergence (dashed line), phonon term (dash-dotted line), and the electronic heat capacity (filled circles) obtained by subtracting the diverging and phonon terms (see text for details). (b) The electronic heat capacities of samples S1 and S2 plotted vs. $T^2$. Solid lines are fits to the $T^2$ dependence in the superconducting state with $T_c$ determined by balancing entropy.

# Extreme magnetic field-boosted superconductivity

Sheng Ran[1,2,3*], I-Lin Liu[1,2,3], Yun Suk Eo[1], Daniel J. Campbell[1], Paul M. Neves[1], Wesley T. Fuhrman[1], Shanta R. Saha[1,2], Christopher Eckberg[1], Hyunsoo Kim[1], David Graf[4], Fedor Balakirev[5], John Singleton[5,6], Johnpierre Paglione[1,2] and Nicholas P. Butch[1,2*]

Nature Physics, 2019

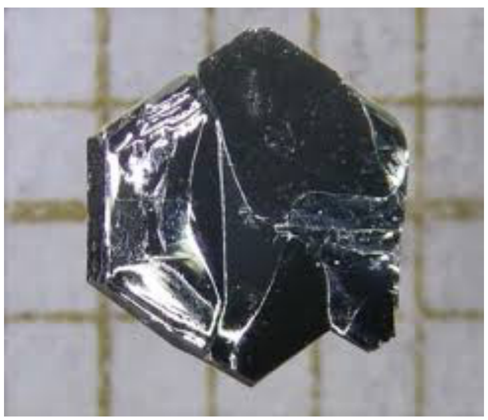

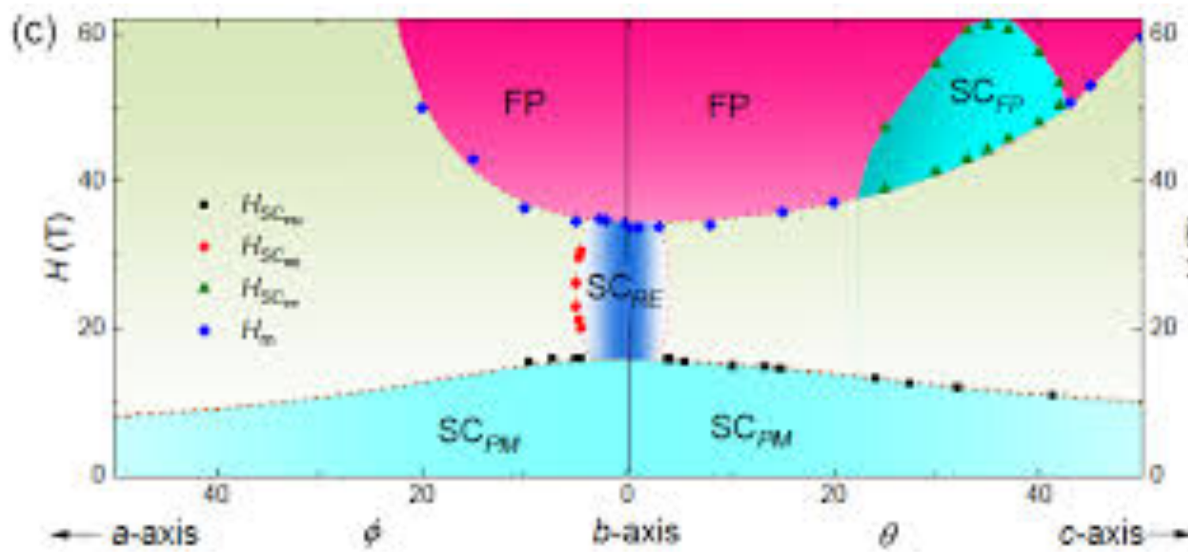


Magnetic field – angle (of field) phase diagram, showing three superconducting phases …

# Computational Methods & Related Data
## Shick & Pickett, PRB 2019

DFT+U calculations; specifically, LSDA+U+SOC

Full potential LAPW code
  Shick & Pickett, PRL 86, 300 (2001)

Fully anisotropic, rotationally invariant functional
  with Hubbard U, Hund's J.   U=0.5 eV = J.
  ["orbital polarization DFT+U" → DFT+U(OP)]

SOC energy scale: in $\xi_{5f}$ **s*l** term, $\xi_{5f}$=220 meV.
  5/2 – 7/2 splitting is 0.77 eV. *Strong* SOC.

Structure: *Immm*, inversion is present.

If Te *s-p* bands are filled: $Te^{2-}$ → *formally* $U^{4+}$ $f^2$.
  Calculated 5f charge in U sphere: $n_f$=2.8.

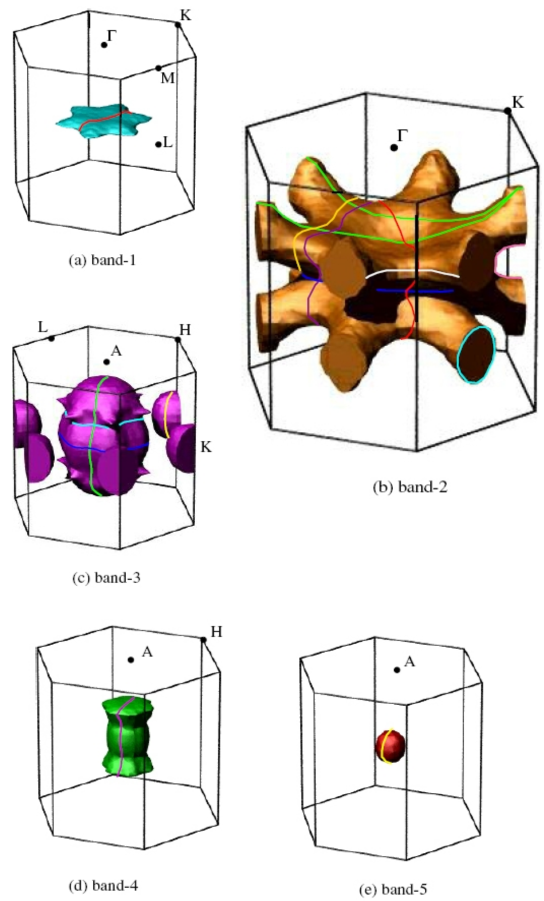


Figure 1. The Fermi surface and f-valence electron count of UPt3
G J McMullan et al 2008 New J. Phys.

UPt3: Heavy Fermion Superconductor

**Fermi surface of UPt3 within the local-density approximation**
*Wang C S, Norman M R, Albers R C, Boring A M, Pickett W E, Krakauer H and Christensen N E*
*1987 Phys. Rev. B* ***35*** *7260*

LDA(!) gives the multi-sheeted Fermi surface of UPt3 correctly.

LDA gives the simpler Fermi surface of $UPd_3$ reasonably only if the occupied 5f orbitals are localized.

**Treatment of U 5f orbitals / bands is a delicate matter.**

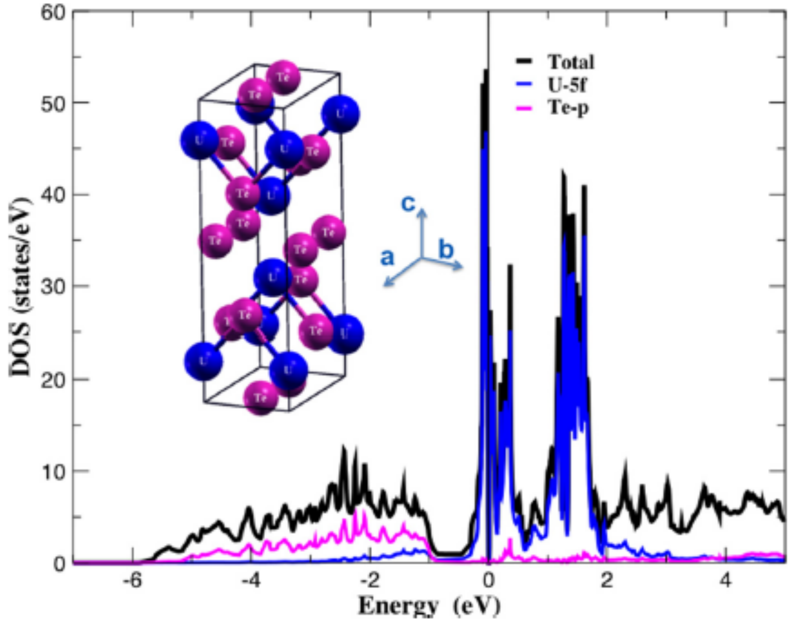


FIG. 1. Total and projected densities of states/eV (per unit cell) for nonmagnetic $UTe_2$ from the local spin density approximation plus Hubbard $U$ [LSDA + $U$(OP)] functional, showing the total (black) and projections for U $5f$ (blue) and Te $5p$ (magenta). The *Immm* $UTe_2$ crystal structure is shown in the inset: blue spheres are U, and magenta spheres are Te. Note that the states near the Fermi level $E_F = 0$ are entirely U $5f$ in character.

Non-magnetic DFT+U(OP) atom-projected DOS

Non-magnetic DFT+U(OP) band structure

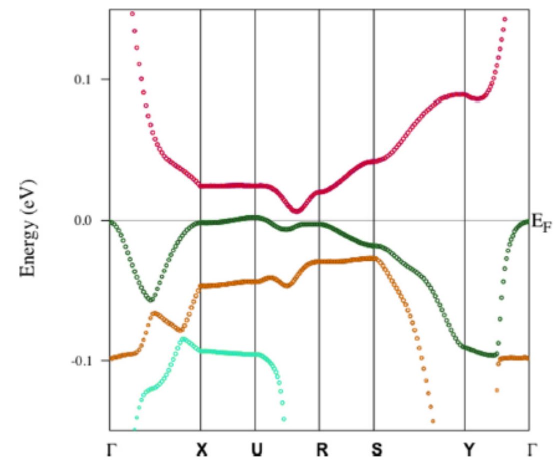


FIG. 2. The band structure from nonmagnetic LSDA+$U$(OP) calculations, which is essentially unchanged from the LSDA bands (the high-symmetry $k$ points $\Gamma[0,0,0]$, $X[\pi/a,0,0]$, $U[\pi/a,0,\pi/c]$, $R[\pi/a,\pi/b,\pi/c]$, $S[\pi/a,\pi/b,0]$, $Y[0,\pi/b,0]$ [23] were used). Without magnetism there is a 13-meV gap. The colors simply distinguish the bands. The circle size, which indicates the amount of $f$ character of the eigenstates, is uniform in this region because the states are uniformly and almost totally U $5f$ in character, consistent with Fig. 1.

Earlier: Aoki et al. JPSJ 2019: LDA

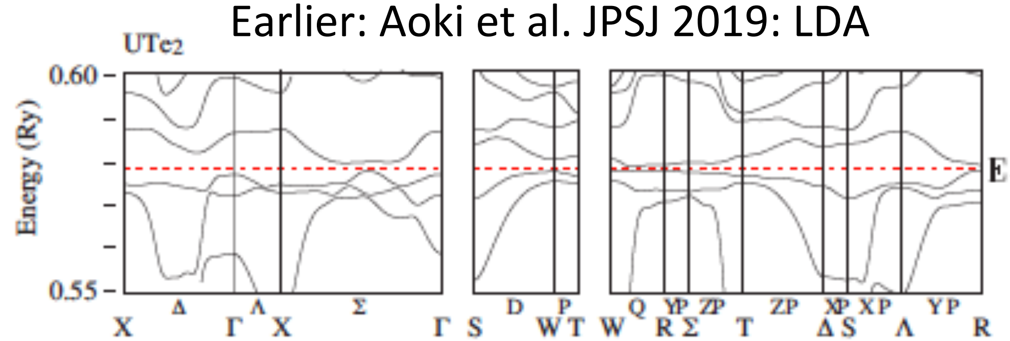

# Electronic Structure of $UTe_2$ Studied by Photoelectron Spectroscopy

Shin-ichi Fujimori[1] *, Ikuto Kawasaki[1], Yukiharu Takeda[1], Hiroshi Yamagami[1,2], Ai Nakamura[3]
Yoshiya Homma[3], and Dai Aoki[3]

JPSJ

LAPW; von Barth-Hedin XC fn'al.
Nonmagnetic.

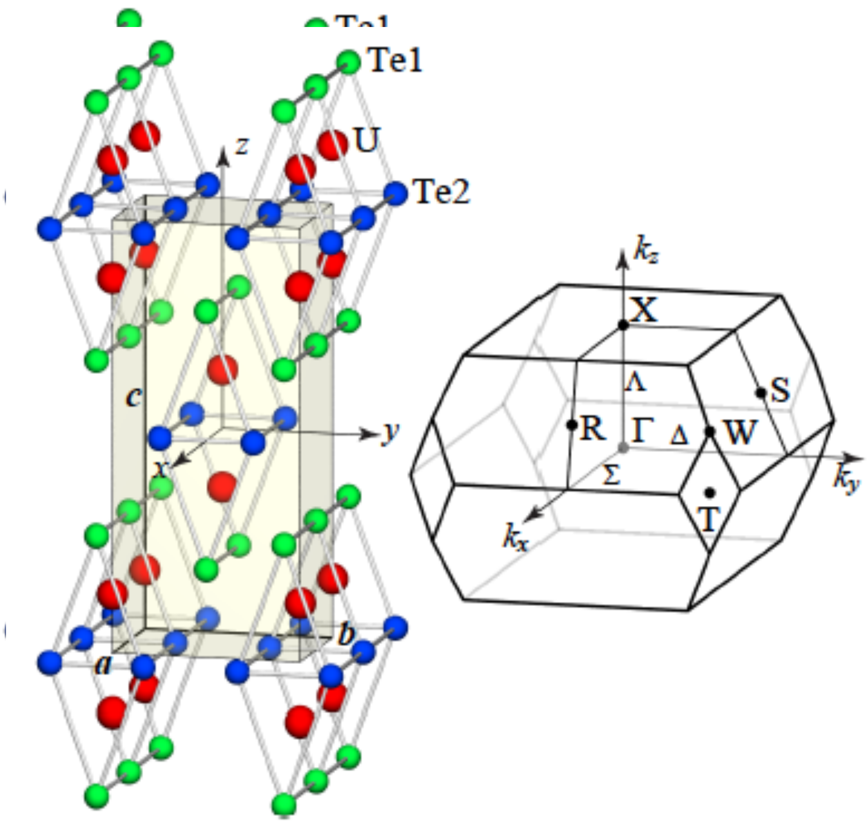


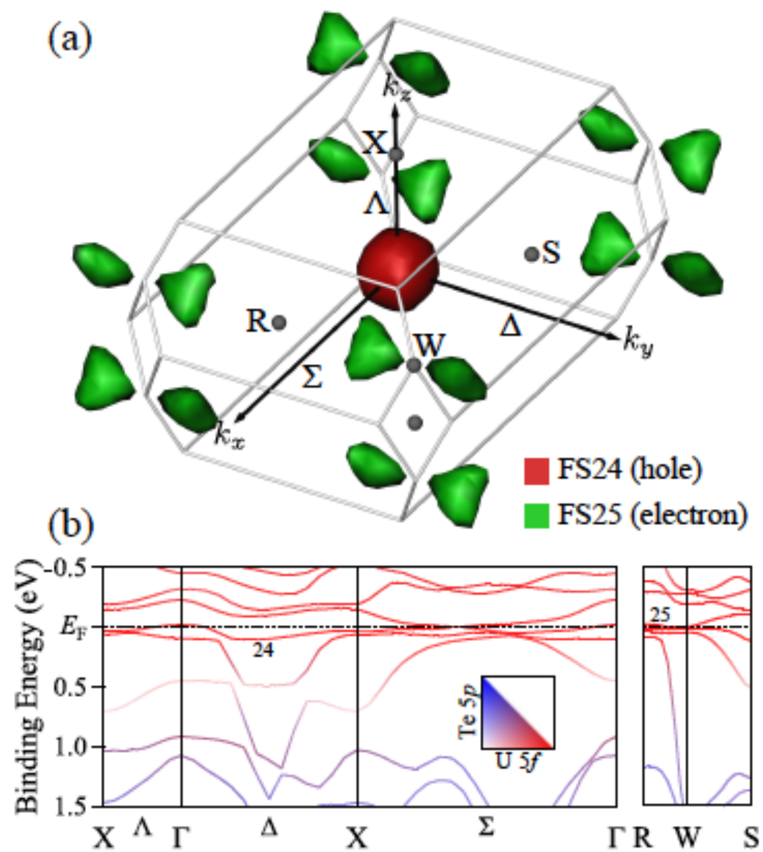

# Insulator-metal transition and topological superconductivity in $UTe_2$ from a first-principles calculation

Jun Ishizuka, Shuntaro Sumita, Akito Daido, and Youichi Yanase

arXiv:1908.04004

Unpolarized DFT+U results

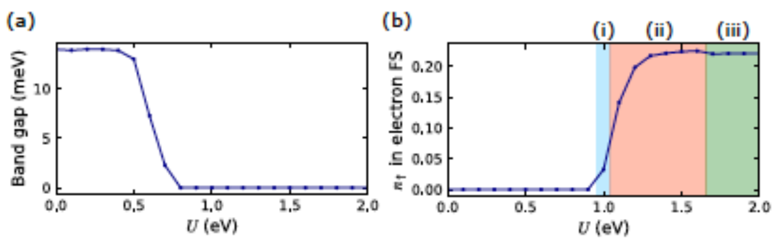


FIG. 1. Coulomb interaction dependence of (a) the band gap at the Fermi level and (b) the electron number $n$ per spin in electron FS. Insulator-metal transition occurs at $U = 1.0$ eV. Metallic states with different topology of FSs are labeled by (i)-(iii).

DFT+U+SOC: varying U

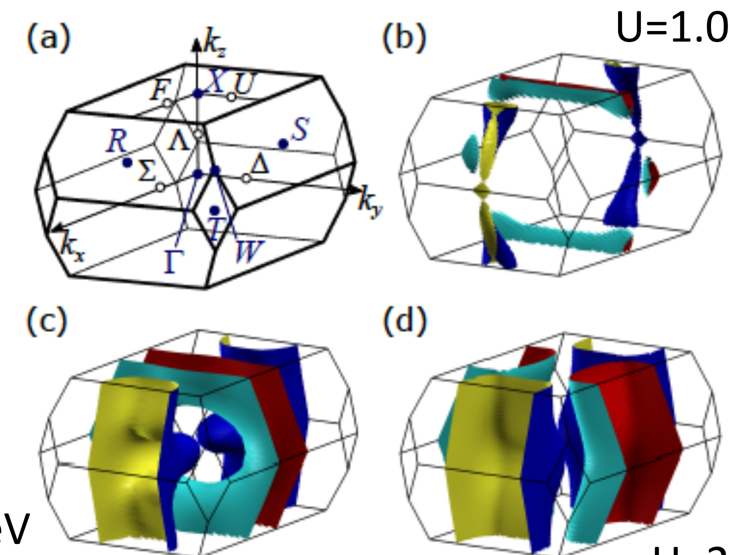


U=1.0 eV

U=1.1 eV

U=2.0 eV

FIG. 2. (a) First BZ and symmetry points. (b)-(d) FSs of $UTe_2$ by GGA+$U$ for (b) $U = 1.0$ eV [region (i)], (c) $U = 1.1$ eV [region (ii)], and (d) $U = 2.0$ eV [region (iii)]. The electron sheet (cyan and red colors) and the hole sheet (blue and yellow colors).

“Nearly an Ising ferromagnet.”
Suppose UTe2 is locally FM at low T.

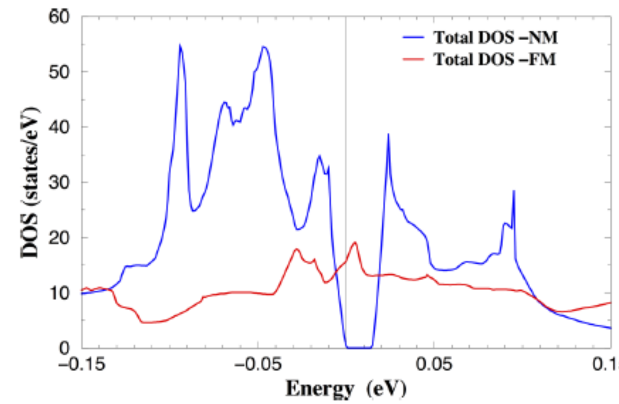


Density of states.
Non-magnetic: small gap.
Ferro: gap completely filled in.

*$UTe_2$ wanted to be a small gap semiconductor.*
*Magnetism destroyed this dream,*
*and led to Kondo physics & superconductivity.*

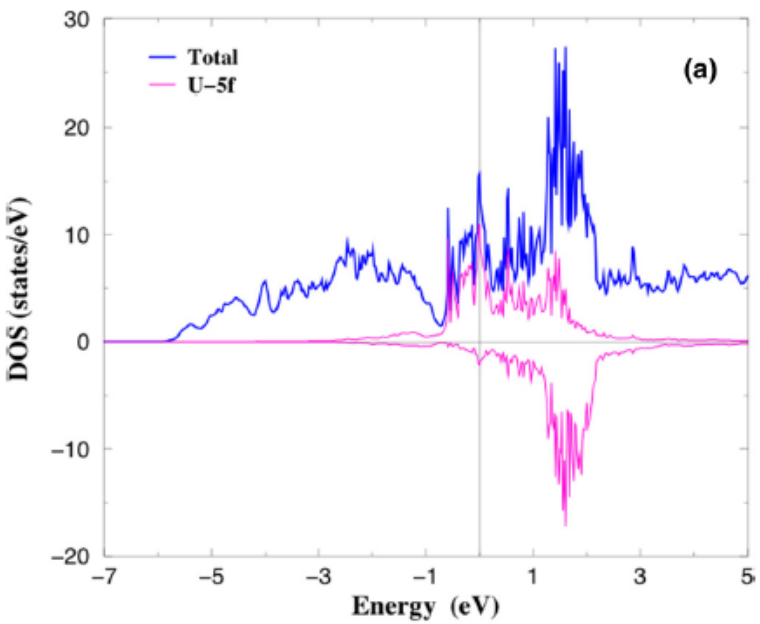


**Spin-projected DOS** for
FM-aligned U moments.

N.B. UTe2 is nearly half-metallic
(fully spin-polarized).
moment ~ $2.8\mu_B$

Unocc. minority 5f bands
are 1.5 eV above $E_F$, “localized”

# Importance of SOC

(Y. Quan)

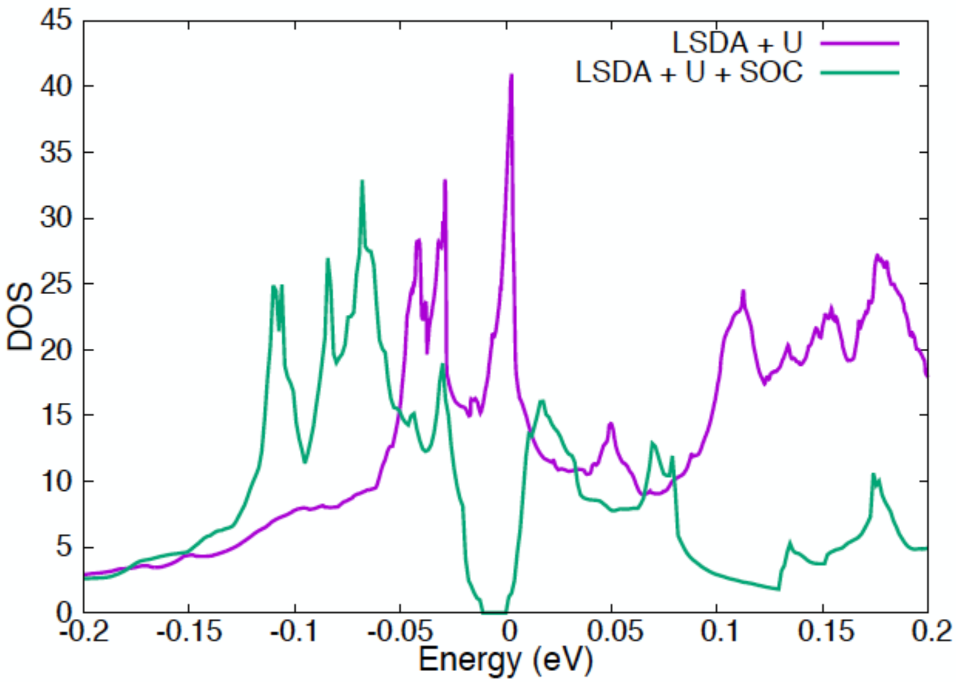


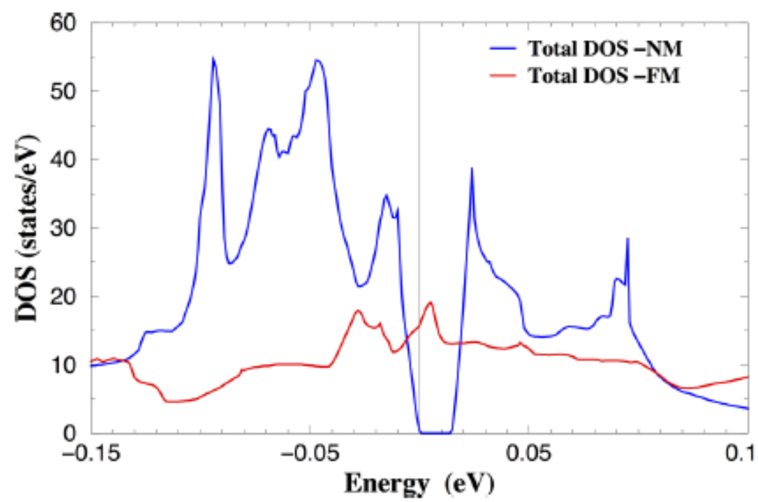


The gap in nonmagnetic $UTe_2$ is generated by SOC.

Then destroyed by magnetism.
Then Kondo physics.
Then superconductivity.
Leaving behind local excitations and associated entropy.

# Different projections of the DOS: FM DFT+U(OP)

Spin-projected DOS

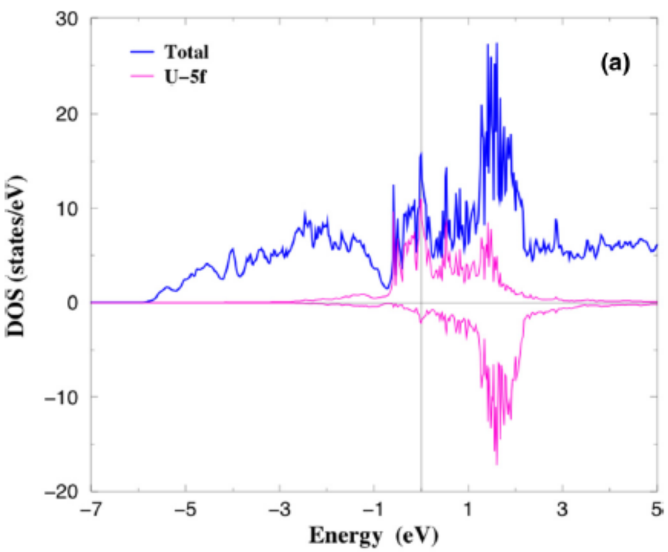


$m_j$-projected DOS.
Much more detail.

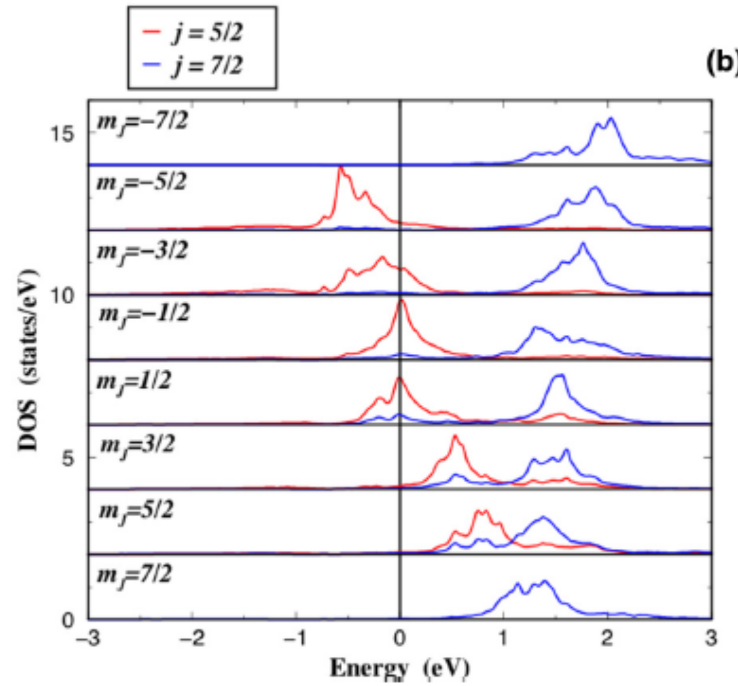


$m_j$=-5/2 and -3/2 are occupied; “local moment”.
**$m_j$=-1/2 and +1/2 are half-filled (instability??)**

# Selected DFT+U(OP) results

*a* is the easy axis. Directing the FM moment along *b* and *c* axes costs 37 meV/U and 96 meV/U respectively. Consistent with experiment; highly anisotropic.

$m_j$ = -5/2 and -3/2 states are fully occupied. "localized moment"

$m_j$= -1/2 and +1/2 are each half-filled, hence unstable against symmetry breaking.

$m_j$ = -+1/2 and -1/2 are

$$\phi_{\frac{5}{2},+\frac{1}{2}} = -\sqrt{\frac{3}{7}}Y_{3,0}|\uparrow\rangle + \sqrt{\frac{4}{7}}Y_{3,+1}|\downarrow\rangle$$

$$\phi_{\frac{5}{2},-\frac{1}{2}} = -\sqrt{\frac{3}{7}}Y_{3,-1}|\uparrow\rangle + \sqrt{\frac{4}{7}}Y_{3,0}|\downarrow\rangle$$

An equal combination leads to (β=+/- 1)

$$\begin{aligned}\Phi_\pm &= \left[\sqrt{\frac{4}{7}}\phi_{\frac{5}{2},+\frac{1}{2}} \pm \beta\sqrt{\frac{3}{7}}\phi_{\frac{5}{2},-\frac{1}{2}}\right] \\ &= \left[\sqrt{\frac{16}{49}}Y_{3,+1}|\downarrow\rangle \mp \beta\sqrt{\frac{9}{49}}Y_{3,-1}|\uparrow\rangle\right] \\ &\quad + \sqrt{\frac{24}{49}}Y_{3,0}\frac{[-|\uparrow\rangle \pm \beta|\downarrow\rangle]}{\sqrt{2}},\end{aligned}$$

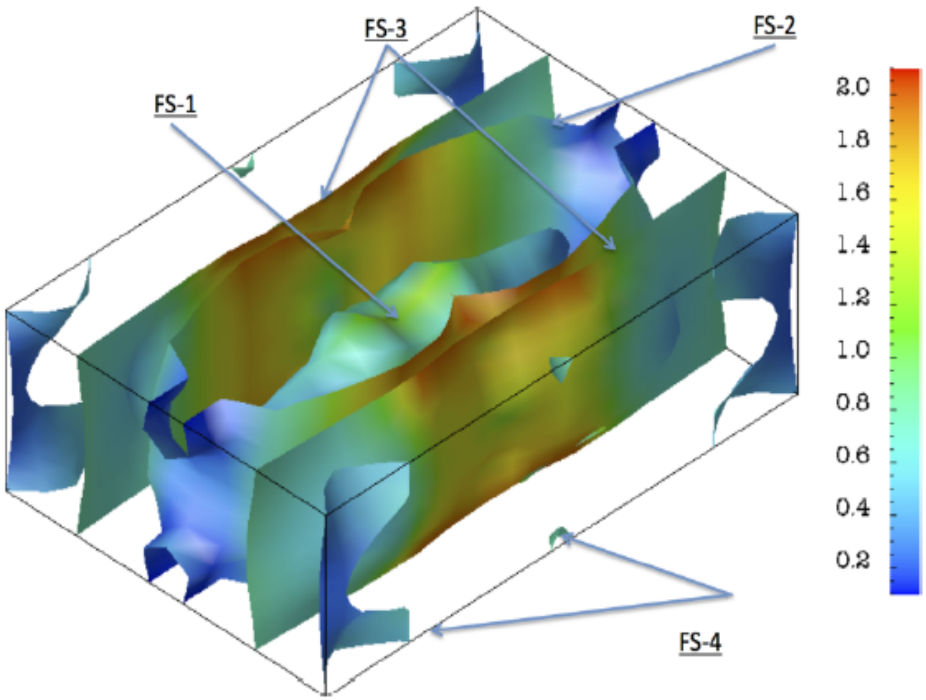


FIG. 5. Fermi surface for FM order, from LSDA+$U$(OP), centered at the Γ point. The Fermi surface is large and multisheeted, with a nesting feature for FS-3 near $(0, \frac{\pi}{b}, 0)$. FS-1 is in the center; FS-2 parallels FS-3 along parts of its length. The low velocities, given by the colorbar, extend over at least an order of magnitude, up to nearly 2 eV/Å ($\sim 2.5 \times 10^7$ cm/s).

# Strong Ising character → $UTe_2$ is locally FM at low temperature

(better than ignoring the Uranium moments)

- multisheeted (multiband)
- some nesting features, mainly around (0,π/b,0) (quasi-1D sheets)
- velocities extend over an order of magnitude (i.e. some v. low velocities)

## Summary: many opportunities for theory in $UTe_2$

- underlying non-magnetic band structure
- near-FM Ising-like magnetic behavior.
  what inhibits magnetic ordering?
- Kondo lattice renormalization to heavy Fermi liquid
- renormalized Fermi surface (?)
- SC gap function / symmetry
- residual entropy, energy scale $\varepsilon \leq 10\ \mu eV$
- effect of B-field, pressure, strain, …

# Calculated moments, restricted to axes.

$\vec{M} \parallel \hat{a}$: $M_S = 1.92\mu_B$, $M_L = -3.44\mu_B$, $M_J = -1.52\mu_B$,
$\vec{M} \parallel \hat{b}$: $M_S = 1.83\mu_B$, $M_L = -3.71\mu_B$, $M_J = -1.88\mu_B$,
$\vec{M} \parallel \hat{c}$: $M_S = 1.91\mu_B$, $M_L = -3.97\mu_B$, $M_J = -2.06\mu_B$.

An analogous calculation for FM $UGe_2$ gave $M_S = 1.32\mu_B$, $M_L = -2.92\mu_B$, and $M_J = -1.58\mu_B$, which was in good agreement with experimental data [25] in the ordered state.

# Calculated MCA Energies:

moment along a: 0 meV
moment along b: 37 meV
moment along c: 96 meV

# Data on UTe2 (ca. early 2019)

*Immm*
bco
space
group
(#71)

Cleaved
surface

Kondo
resonance
of heavy
Fermi
liquid

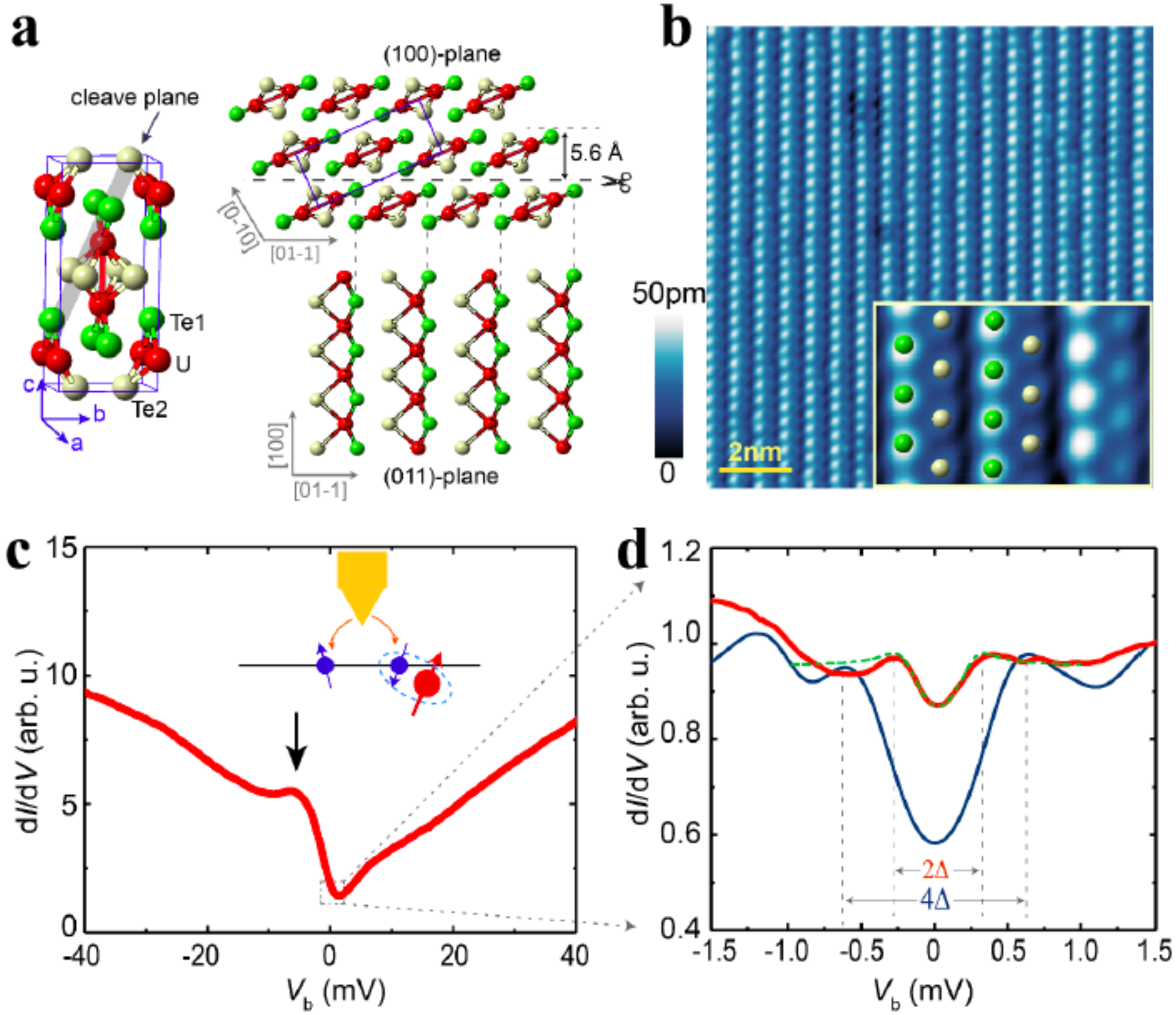


dI/dV curves:
normal tip;
sc'ing tip

…chiral superconducting order parameter in heavy fermion UTe2,
Jiao et al., 2019

# $UTe_2$: A New Spin-Triplet Pairing Superconductor

**Anne de Visser** **JPSJ News and Comments 16, 08 (2019)**

Table I: Superconducting ferromagnets and their characteristic parameters: Curie temperature, $T_C$, superconducting transition temperature, $T_{sc}$, ordered moment, $m_0$, Curie–Weiss effective moment, $p_{eff}$, and linear coefficient in the specific heat, $\gamma$. In the last row is listed $UTe_2$, a superconductor at the verge of ferromagnetic order.

| Material | Structure | $T_C$ (K) | $T_{sc}$ (K) | $m_0$ ($\mu_B$/U atom) | $p_{eff}$ ($\mu_B$/U atom) | $\gamma$ (J/mol $K^2$) | Ref. |
|---|---|---|---|---|---|---|---|
| $UGe_2$ | orthorhombic | 53 | 0.8[a] | 1.5 ‖ *a* | 2.9 | 0.032 | 1 |
| URhGe | orthorhombic | 9.5 | 0.25 | 0.42 ‖ *c* | 1.8 | 0.160 | 2 |
| UIr | monoclinic | 46 | 0.1[b] | 0.50 ‖ $[10\bar{1}]$ | 2.4 | 0.049 | 3 |
| UCoGe | orthorhombic | 3 | 0.6 | 0.07 ‖ *c* | 1.7 | 0.057 | 4 |
| $UTe_2$ | orthorhombic | →0 | 1.6 | →0 | 2.8 | 0.117 | 5 |

[a]at a pressure of 1.2 GPa; [b]at a pressure of 2.7 GPa

# Ferromagnetic Superconductors

Rare: (singlet) superconductors hate magnetic fields

- expel magnetic fields; entirely, or into vortices
- superconducting magnetic levitation

Central fact: magnetic source is strong compared to sc'y,

and the source of the B field is dense within the material

Central issue: how does superconducting state cope with the field?

- by pairing in a triplet state, rather then singlet.

UGe2,
UCoGe,
URhGe
UIr

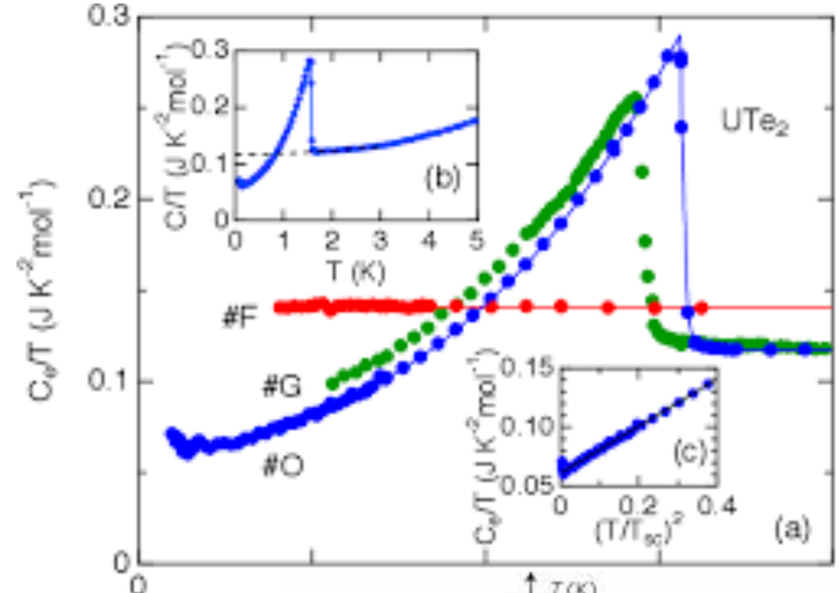
0.3
0.2
0.1
0
0
$C_e/T$ (J K$^{-2}$mol$^{-1}$)
UTe$_2$
#F
#G
#O
(a)
$C/T$ (J K$^{-2}$mol$^{-1}$)
0.3
0.2
0.1
0
0 1 2 3 4 5
T (K)
(b)
$C_e/T$ (J K$^{-2}$mol$^{-1}$)
0.15
0.10
0.05
0 0.2 0.4
$(T/T_{sc})^2$
(c)

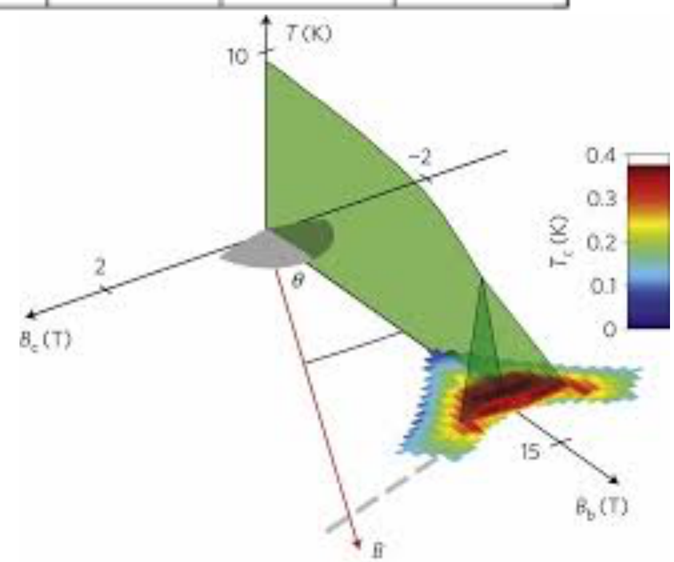
T (K)
10
−2
2
$B_c$ (T)
θ
15
$B_b$ (T)
B
$T_c$ (K)
0.4
0.3
0.2
0.1
0